Geological Society of America
Special Paper 419
2007

The Maksyutov Complex: The first UHP terrane 40 years later

Rachel Beane[†]
Department of Geology, Bowdoin College, 6800 College Station, Brunswick, Maine 04011, USA

Mary Leech[‡]
Department of Geological and Environmental Sciences, Stanford University, Stanford, California 94305-2115, USA

ABSTRACT

Radial fractures around quartz inclusions in garnets from the Maksyutov Complex were first described nearly 20 years before coesite in crustal rocks was recognized elsewhere as evidence for ultrahigh-pressure (UHP) metamorphism and deep (>90 km) subduction. Twenty years later, evidence for microdiamond in garnet was described in the Maksyutov Complex. The intervening 40 years brought researchers from around the world to the south Ural Mountains of Russia to investigate the petrology, geochemistry, structure, and geochronology of the Maksyutov Complex. The well-studied Maksyutov Complex provides insights into the exhumation processes of UHP terranes.

The protolith of the UHP Kairakli unit of the Maksyutov Complex began as Cambrian rift-induced basalt intruded into Proterozoic metasedimentary rocks of the East European platform. The Kairakli unit was subducted eastward beneath the forming Magnitogorsk island arc and metamorphosed at 650 °C and 2.6–3.2 GPa at ca. 385 Ma. Synconvergent buoyant exhumation brought the Kairakli unit to lower-crustal depths, where shear zones juxtaposed it with the meta-ophiolite-bearing Karamola unit and an intervening sedimentary unit, the Yumaguzino quartzite, at ca. 360 Ma. By 315 Ma, all units were exhumed to 3–4 km depth.

Exhumation rates for the Maksyutov Complex of 5 mm/yr are much slower than the ~25 mm/yr estimated for other UHP terranes. This calculated rate supports research that found fast exhumation rates are not the most efficient means to cool a UHP terrane so as to preserve coesite or microdiamond. Instead, the Maksyutov Complex, a thin slab (<10 km), probably was kept cool by continued subduction of cold crust during its buoyant exhumation.

Keywords: ultrahigh-pressure metamorphism, Ural Mountains, geochronology, geochemistry, exhumation.

[†]E-mail: rbeane@bowdoin.edu.
[‡]Present address: Department of Geosciences, San Francisco State University, San Francisco, California 94132, USA; e-mail: leech@sfsu.edu.

Beane, R., and Leech, M., 2007, The Maksyutov Complex: The first UHP terrane 40 years later, *in* Cloos, M., Carlson, W.D., Gilbert, M.C., Liou, J.G., and Sorensen, S.S., eds., Convergent Margin Terranes and Associated Regions: A Tribute to W.G. Ernst: Geological Society of America Special Paper 419, p. 153–169, doi: 10.1130/2006.2419(08).

INTRODUCTION

Ultrahigh-pressure (UHP) metamorphism refers to the metamorphism of crustal rocks at pressures high enough to crystallize the index minerals coesite (a high-pressure polymorph of quartz requiring $P > 2.7$ GPa at $T > 600$ °C) or diamond. Prior to the initial discoveries of coesite in supracrustal rocks (Chopin, 1984; Smith, 1984), coesite and diamond were thought to occur only in meteorite-impact craters and mantle xenoliths. The discovery of upper-crustal rocks metamorphosed at ultrahigh pressure changed the understanding of crustal-scale processes in continental collision zones (cf. Liou et al., 1994; Coleman and Wang, 1995; Hacker and Liou, 1998; Ernst and Liou, 2000; Liou et al., 2004) by challenging existing views about subduction, exhumation, continental collision and growth, and crust-mantle interactions.

Thus far, more than a dozen UHP terranes have been documented in Eurasian continental collision orogens (cf. Ernst and Liou, 2000; Liou et al., 2004). These terranes formed during aborted subduction to depths of 135 km or more (within the diamond stability field) and share common structural and lithological characteristics, for instance: (1) Records of UHP metamorphism occur as coesite inclusions in garnet, zircon, and omphacite, and as microdiamonds in garnet and zircon, mainly in eclogites and garnet peridotites included as pods and slabs within quartzofeldspathic gneisses; (2) the host rocks are of continental and subcontinental geochemical and petrological affinities; and (3) the exhumed UHP metamorphic rocks occur in a supracrustal setting as multiple-kilometer-thick slabs bounded above by normal faults (e.g., Hacker et al., 2000) and below by reverse faults.

Forty years ago, Chesnokov and Popov (1965) described radial cracks system around quartz inclusions in garnet, omphacite, and glaucophane from crustal rocks in the Maksyutov Complex, south Urals, Russia (Fig. 1). After Chopin (1984) and Smith (1984) associated coesite-bearing crustal rocks with UHP metamorphism and deep subduction, one interpretation put forward by Chesnokov and Popov (1965), i.e., that Maksyutov Complex rocks may once have contained coesite, gained plausibility. More than 30 papers and many more abstracts have been published on the petrology, geochronology, and evolution of the Maksyutov Complex. This paper summarizes the research in recent papers and earlier Russian literature, to provide an overview of the Maksyutov Complex and to draw attention to its potential significance in our understanding of orogens and the evolution of UHP terranes.

The Maksyutov Complex is a subduction zone metamorphic terrane that formed upon the closure of the Uralian Ocean during the late Paleozoic. It is situated in the southernmost portion of the ~2500 km long Uralide orogen, which separates Europe and Asia. The Uralide orogen formed during Late Devonian to Permian collisions among the East European platform (to the west), the intervening Magnitogorsk island arc, and microcontinental blocks (to the east; Zonenshain et al., 1990). The southern portion of the orogen shows no evidence for postorogenic extensional collapse (Berzin et al., 1996; Echtler, 1996; Knapp et al., 1998; Leech, 2001) and preserves the late Paleozoic collisional structure. This paper will review the structural and lithological characteristics of the Maksyutov Complex, including evidence for UHP metamorphism, the petrology and geochemistry of the host rocks, and the structural, geochronologic, and thermal data that lead to exhumation models.

REGIONAL GEOLOGY

The Main Uralian fault is the major arc-continent suture in the Uralide orogen, extending 2500 km along the axis of the ~400 km wide orogen (Fig. 1) (Zonenshain et al., 1984, 1990). As supported by the URSEIS (Urals Reflection Seismic Experiment and Integrated Studies) project, the east-dipping thrust fault is widely interpreted to separate the East European platform in the west from the accreted Siberian-Kazakhian terrane assemblage to the east (cf. Brown et al., 1998; Hetzel and Romer, 2000; Hamilton, 1970). A generally west-vergent thrust stack constitutes the footwall beneath the Main Uralian fault in the south Uralide orogen (Fig. 1C) (Brown et al., 1998; Brown and Spadea, 1999). The Maksyutov Complex, formed during the eastward subduction of the East European continental margin, is in the upper part of this thrust stack (Beane and Connelly, 2000; Brown et al., 1998). The Maksyutov Complex is bounded on its western margin by the Yantyshevo-Yuluk fault that backthrusts greenschist-facies metasediments of the Suvanjak Complex eastward over the Maksyutov Complex (Brown et al., 1998; Chibrikova and Olli, 1994). To the east of the Maksyutov Complex, the Magnitogorsk island arc, sometimes referred to as Irendyk (Zonenshain et al., 1984; Hetzel et al., 1998), is in the hanging wall of the Main Uralian fault. The basement of the Magnitogorsk island-arc complex is ophiolites, overlain by Early to Middle Devonian island-arc volcanic rocks, and topped by Middle to Late Devonian forearc basin sediments (Zonenshain et al., 1984; Savelieva and Nesbitt, 1996). East of the Magnitogorsk island-arc complex are the Vendian-Ordovician Mugodzhar and Ilmen microcontinents intruded by Late Carboniferous–Permian granitic plutons (Zonenshain et al., 1990; Bea et al., 2002).

Seismic reflection data suggest that the Moho of the south Uralide orogen is at a depth of ~55 km (Knapp et al., 1998; Berzin et al., 1996; Carbonell et al., 1996; Echtler, 1996). Under the central axis of the Urals the Moho is diffuse, possibly a result of an eclogitized root (Knapp et al., 1998) or partial eclogitization of lower-crustal rocks (Leech, 2001). The continuity of the low surface topography (<1600 m) and the great depth of the crustal root signify that the Uralide orogen has preserved its collisional structure from the late Paleozoic, with no evidence of postorogenic tectonic collapse (Leech, 2001; Knapp et al., 1998; Berzin et al., 1996; Echtler, 1996).

DESIGNATION AND PETROLOGY OF MAKSYUTOV COMPLEX UNITS

The Maksyutov Complex, as exposed, is a 15–20 km wide, ~150 km long belt (Beane et al., 1995; Lennykh et al., 1995; Hetzel et al., 1998) with a structural thickness of 5–10 km

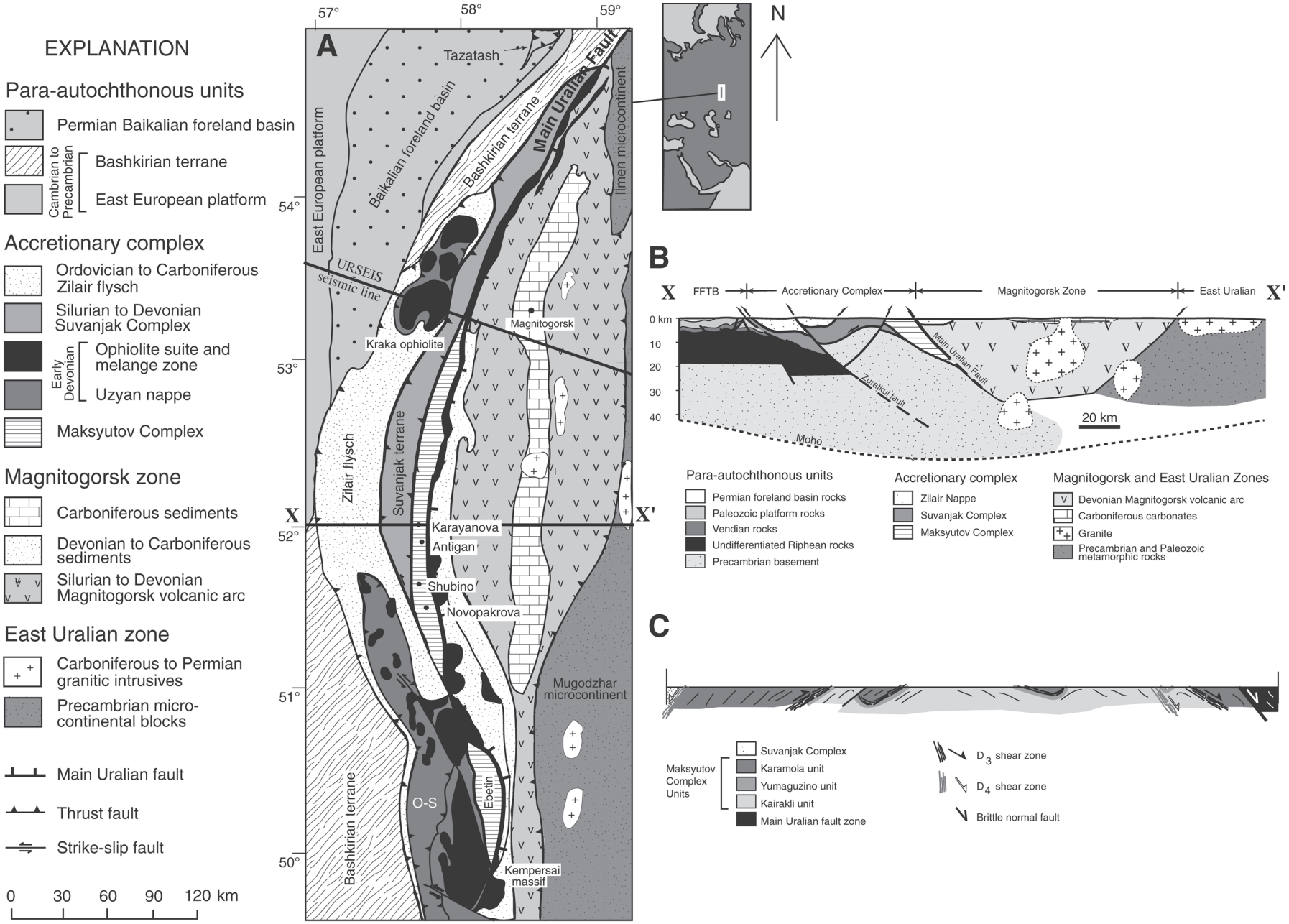

Figure 1. (A) Tectonostratigraphic map of the south Ural Mountains (after Leech and Stockli, 2000) with sampling areas that are mentioned in the text and Table 1. (B) Crustal-scale cross section X–X′ through the south Urals based on Brown et al. (1998). FFTB—foreland fold-and-thrust belt. (C) East-west cross section of the Maksyutov Complex at Antigan (modified after Hetzel et al., 1998) showing the structural relationship between the different units.

(Dobretsov, 1974; Hetzel et al., 1998; Leech and Willingshofer, 2004). The subdivisions of the Maksyutov Complex have been designated in various ways over the past 50 years, some names based on metamorphic grade (cf. Klochichin and Burychenko, 1957; Beane et al., 1995), others lithostratigraphically defined (cf. Krinizky and Krinizkaya, 1961; Lennykh, 1977), and some defined by structural position (cf. Valizer and Lennykh, 1988; Lennykh et al., 1995; Leech and Ernst, 1998; Hetzel and Romer, 2000). Hetzel (1999) provides a table that correlates most designations. Recent work has defined two subdivisions by structural position, using terms such as "upper unit 2" and "lower unit 1" (cf. Hetzel and Romer, 2000; Bostick et al., 2003). Although this designation is convenient for western geologists, it ignores the "middle unit," differs from the typical way geologists name units, and does not credit the early stratigraphic work of Russian geologists. Accordingly, we use the lithostratigraphic names (Krinizky and Krinizkaya, 1961; Gorochov and Chabakov, 1961; Alekseyev, 1976) given to the units in the Maksyutov Complex. Descriptions of the units follow.

Kairakli Unit

The Kairakli unit, metamorphosed under UHP eclogite-facies conditions consists of volumetrically minor blocks or boudins of mafic eclogite, talc-enstatite, olivine-enstatite, and jadeite-quartzite in a matrix of metasedimentary rocks (Figs. 2A and 2B) (Dobretsov, 1974; Dobretsov et al., 1996; Beane et al., 1995; Hetzel et al., 1998). Petrologic descriptions of the rock types are given by Dobretsov et al. (1996). Three stages of metamorphism are observed in mafic eclogite: M_1 (eclogite-facies; Fig. 3A) garnet + omphacite + phengite + quartz + rutile; M_2 (blueschist-facies; Fig. 3B) garnet + glaucophane ± lawsonite ± titanite; and M_3 (greenschist-facies) epidote + chlorite ± albite ± actinolite (Beane et al., 1995; Lennykh et al., 1995; Hetzel, 1999; Schulte and Blümel, 1999). The metasedimentary rocks occur as intensely deformed schist and gneiss, including metapelite, metagraywacke, and graphitic quartzite (Fig. 3C) (Dobretsov et al., 1996; Hetzel et al., 1998; Leech and Ernst, 1998; Alekseev, 2000). The Kairakli unit has been interpreted as a metasedimentary mélange of microcontinental fragments (Dobretsov, 1974; Dobretsov et al., 1996), and more recently as subducted continental crust of the East European platform (Hetzel, 1999) with dikes and sills of basalt (Leech and Ernst, 2000; Volkova et al., 2004) that were transformed to eclogite during subduction.

Yumaguzino Unit

The Yumaguzino unit alternatively is referred to as the "middle unit," or "quartzite unit." This blueschist-facies unit consists of white quartzite with a structural thickness of 600 m (Lennykh et al., 1995). Lenses within the quartzite are rich in phengite, chlorite, feldspar, stilpnomelane, or sodic amphibole (Fig. 3D) (Beane and Connelly, 2000; Hetzel, 1999).

Karamola Unit

The Karamola unit consists of a blueschist/greenschist-facies, serpentinite-matrix mélange, volcanic rocks, marble, and graphite-bearing quartzite (Dobretsov et al., 1996; Beane and Liou, 2005). The discontinuous serpentinite-matrix mélange has 0.5–10 m^2 blocks of chlorite-rich, lawsonite- and garnet-bearing, metasomatized basalts (Lennykh and Valizer, 1986; Schulte and Sindern, 2002; Beane and Liou, 2005). An impressive feature of some of the metasomatized blocks is millimeter- to centimeter-sized pseudomorphs of muscovite, clinozoisite, and garnet after lawsonite (Figs. 2C and 3E), first described by Lodochnikov (1941). Petrologic evidence suggests that Mg-metasomatism of the blocks followed rodingitization during continued serpentinization of surrounding peridotites, leading to chloritization of igneous plagioclase and prevalent Mg-rich rims around the mafic blocks (Beane and Liou, 2005). Late K-metasomatism contributed to the formation of muscovite pseudomorphs after lawsonite (Schulte and Sindern, 2002).

GEOCHEMISTRY

Whole-Rock Geochemistry

Kairakli Unit

The whole-rock geochemical data indicate that eclogites and blueschists derive from dikes and sills of tholeiitic basalt of E-MORB (enriched mid-oceanic-ridge basalt) affinities (Volkova et al., 2004; Leech and Ernst, 2000; Schulte and Blümel, 1999). Oxygen isotopes from metabasalt and surrounding metasedimentary rocks are typical of unaltered protoliths (Leech and Ernst, 2000). Whole-rock compositions of the metabasalt vary with 41–54% SiO_2, 11–18% Al_2O_3, 11–19% Fe_2O_3 (total), <0.4% MnO, 4–13% MgO, 4–14% CaO, 1–5% Na_2O, and <3% K_2O (Volkova et al., 2004; Leech and Ernst, 2000; Schulte and Blümel, 1999). Metabasalts display HFSE (high field strength element) and LREE (light rare earth element) enrichment (La/Lu ratio from 2.7 to 4.8), typical of basalts derived from spreading centers (Volkova et al., 2004).

Based upon 40 analyses of one metabasalt boudin, Volkova et al. (2004) divided rock compositions into three clusters distinguished primarily by MgO content; these authors attributed trace element differences to fractional crystallization and cumulate processes, rather than metamorphic differentiation. Schulte and Blümel (1999) found variations of the Fe_2O_3/MgO ratios of eclogite boudin, foliated eclogite, and garnet-mica schist that they interpreted as differences in protolith. Volkova et al. (2004) found no statistical distinction between eclogite and glaucophane-bearing eclogite.

Karamola Unit

Mafic rocks from the Karamola unit show the chemical effects of Mg-, Ca-, and K-metasomatism (Beane and Liou, 2005; Schulte and Sindern, 2002). Compositions of the least altered

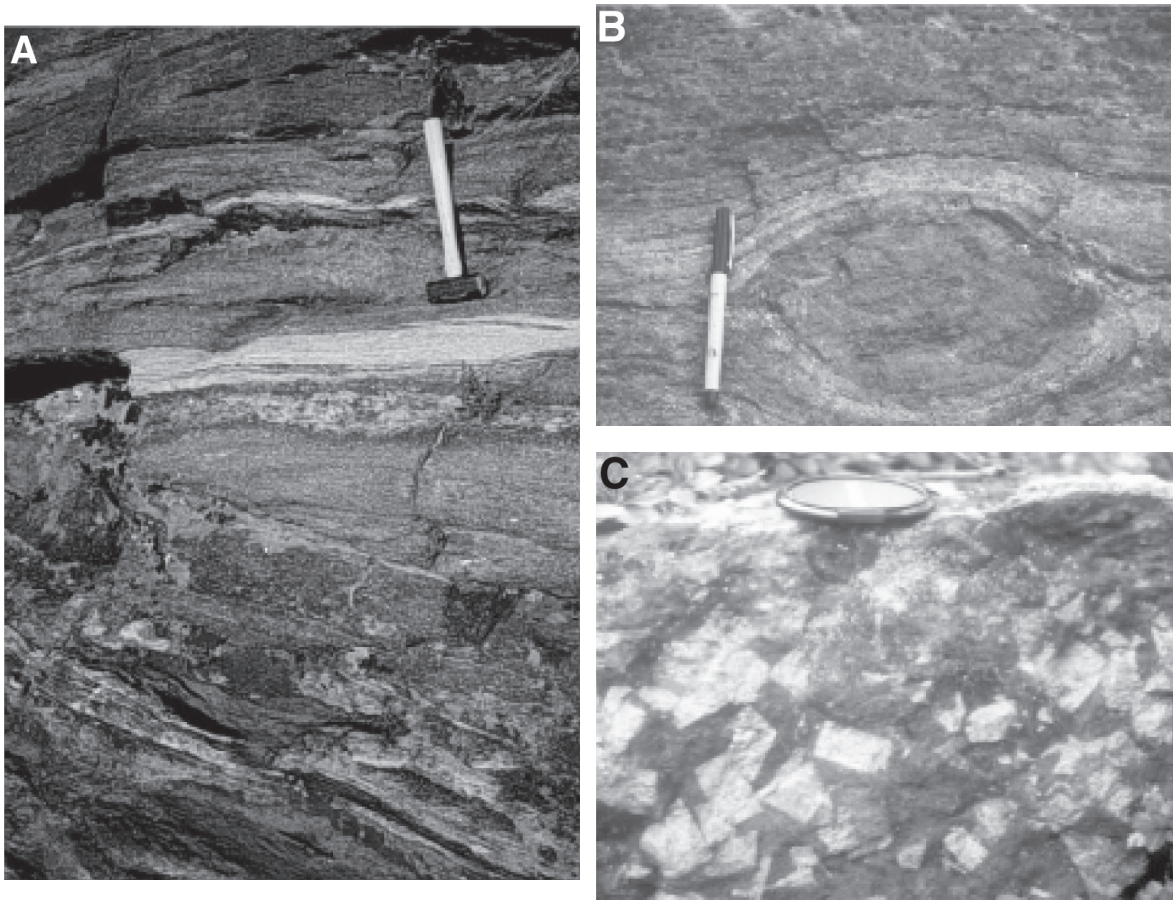

Figure 2. Photographs showing key field relations. (A) Banded gneiss of the Kairakli unit showing blueschist- and eclogite-facies mafic rocks and quartz-rich and mica-rich metasedimentary rocks (hammer for scale). (B) Eclogite boudin in metasedimentary rock of the Kairakli unit (pen for scale). (C) Metasomatized mafic rock of the Karamola unit with rhombic, white pseudomorphs after lawsonite (camera lens cap for scale).

samples resemble metabasalts of the Kairakli unit and, likewise, are interpreted to have derived from E-MORB material (Beane and Liou, 2005). Oxygen isotopes for the metabasalt and surrounding metasedimentary rock of the Karamola unit are comparable to those for the Kairakli unit and therefore also typical of unaltered sediments and oceanic basalt (Leech and Ernst, 2000). The metabasalts exhibit a wide range of major element compositions, which reflect the degree of metasomatism: 27–52% SiO_2, 14–25% Al_2O_3, 7–8% Fe_2O_3 (total), 0.1–3% MnO, 4–13% MgO, 1–18% CaO, 0.1–6% Na_2O, and 0–3% K_2O (Beane and Liou, 2005; Schulte and Sindern, 2002).

Mineral Compositions

Kairakli Unit

Garnet from eclogite boudins is almandine-rich ($Alm_{54–68}$, $Prp_{7–29}$, $Grs_{8–29}$, $Sps_{1–4}$). In some but not all garnets, core-to-rim zoning is observed that shows increased Mg and decreased Mn and Ca contents. Garnets with this zonation may be interpreted to preserve the prograde growth signature (Glodny et al., 2003). Clinopyroxene is omphacitic in composition ($Jd_{39–55}$). White mica is present typically as phengite ($Si_{3.3–3.6}$) and occasionally as paragonite. Epidote in blueschists displays $Ps_{3–29}$, increasing toward the rim. Amphibole compositions are glaucophane and barroisite.

Garnets in metasedimentary rocks display lower almandine components ($Alm_{36–41}$, $Prp_{27–33}$, $Grs_{14–20}$, $Sps_{13–17}$) than those from eclogites. These compositions have been interpreted to reflect differences in bulk composition or variations in *P-T* conditions of metamorphism (Leech and Ernst, 2000; Schulte and Blümel, 1999). White mica again occurs as phengite ($Si_{3.3–3.5}$) or paragonite.

Karamola Unit

Analyses of minerals from metabasalts in the Karamola unit (Beane and Liou, 2005; Schulte and Sindern, 2002; Hetzel et al., 1998) are summarized as follows: (1) Lawsonite typically is pseudomorphosed by Ms ± Grt ± Czo; where preserved, lawsonite has nearly stoichiometric composition with $Si_{2.0}$, $Al_{1.0}$, $Ca_{0.98}$, $Fe^{3+}_{0.01}$; (2) white mica in the matrix and as pseudomorphs after lawsonite

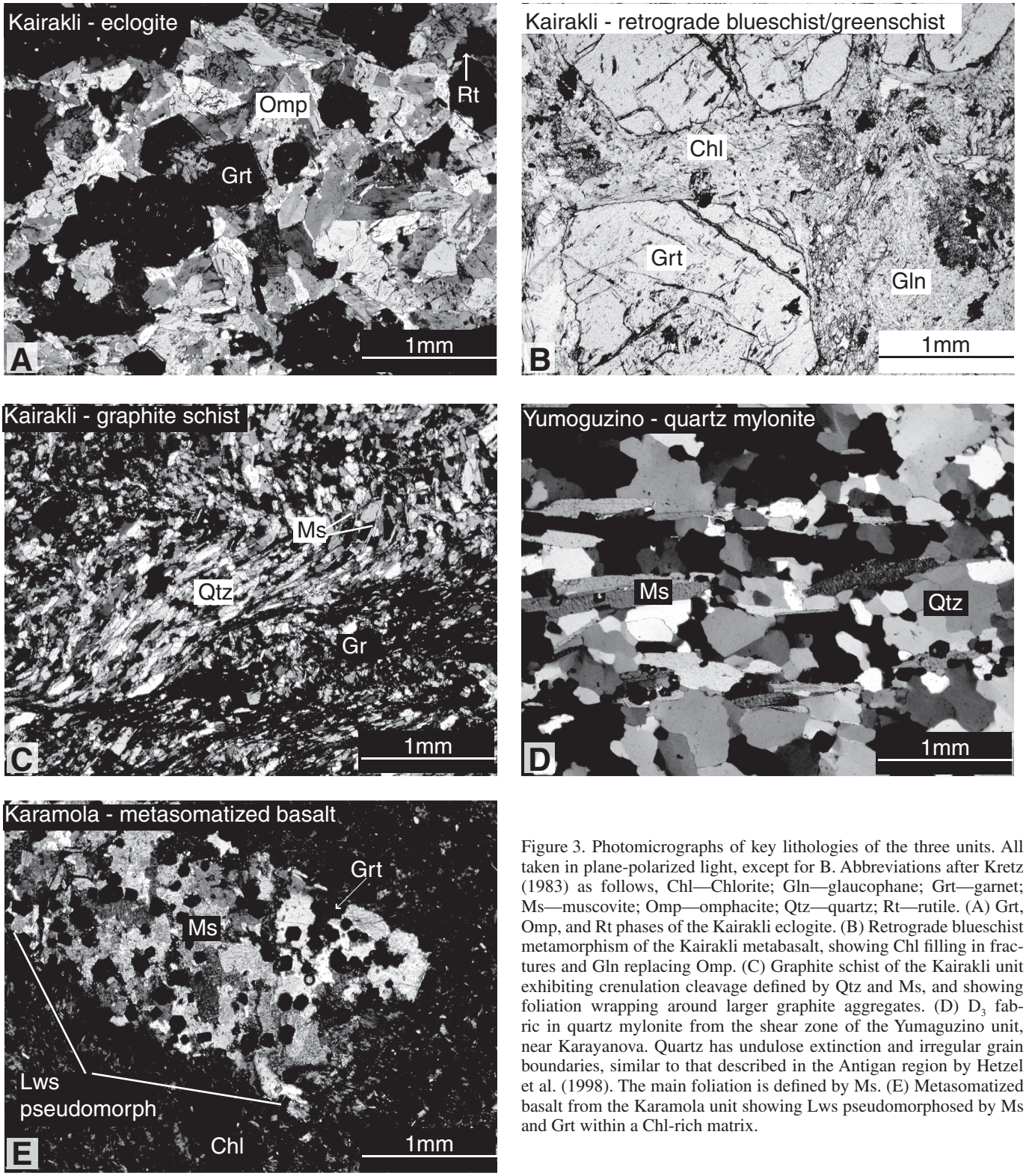

Figure 3. Photomicrographs of key lithologies of the three units. All taken in plane-polarized light, except for B. Abbreviations after Kretz (1983) as follows, Chl—Chlorite; Gln—glaucophane; Grt—garnet; Ms—muscovite; Omp—omphacite; Qtz—quartz; Rt—rutile. (A) Grt, Omp, and Rt phases of the Kairakli eclogite. (B) Retrograde blueschist metamorphism of the Kairakli metabasalt, showing Chl filling in fractures and Gln replacing Omp. (C) Graphite schist of the Kairakli unit exhibiting crenulation cleavage defined by Qtz and Ms, and showing foliation wrapping around larger graphite aggregates. (D) D_3 fabric in quartz mylonite from the shear zone of the Yumaguzino unit, near Karayanova. Quartz has undulose extinction and irregular grain boundaries, similar to that described in the Antigan region by Hetzel et al. (1998). The main foliation is defined by Ms. (E) Metasomatized basalt from the Karamola unit showing Lws pseudomorphosed by Ms and Grt within a Chl-rich matrix.

display ($Si_{3.0–3.2}$) a lower celadonite component than phengite from the Kairakli unit; some white mica is chromium-bearing (Alekseyev et al., 1978; Beane and Liou, 2005); (3) pumpellyite is distinctively Al-rich; (4) garnets are relatively grossular-rich with great variations in spessartine, pyrope, and uvarovite components ($Alm_{1–62}$, $Prp_{1–5}$, $Grs_{20–51}$, $Sps_{0–48}$, $Uv_{0–36}$) that likely reflect the variable metasomatism of these rocks; core-to-rim zoning in garnet shows decreasing Mn content; (5) total Fe in epidote-clinozoisite varies from 0.1% to 0.4%, which is inversely proportional to Al.

THERMOBAROMETRY

Evidence for UHP Metamorphism

The hallmarks of ultrahigh-pressure metamorphism are the index minerals coesite or diamond in crustal rocks. The Kairakli unit of the Maksyutov Complex consists of metasedimentary rocks and eclogites of crustal origin. The documentation of UHP index minerals in this unit has been more elusive. As noted previously, Chesnokov and Popov (1965) described the presence of radial cracks surrounding quartz inclusions in garnet from eclogite near Shubino village (locations shown in Fig. 1A); they offered as an interpretation that the quartz inclusions were pseudomorphs after coesite. Dobretsov and Dobretsova (1988) reported relict coesite in jadeite-quartzite from the Karayanova area, describing radiating microfractures in garnet and a blue glow to the inclusions under an electron microprobe beam; the small size of the inclusions precluded Raman identification. Other workers studied hundreds of thin sections and failed to identify coesite (Matte et al., 1993; Beane et al., 1995; Hetzel et al., 1998). Then, Leech and Ernst (1998) described millimeter- to centimeter-scale cuboid graphite aggregates in schists from Karayanova. The dominant foliation within the schist wraps around these aggregates. Such pressure shadows indicate that during the deformation that created the foliation, the graphite aggregates behaved rigidly. Because graphite deforms easily, Leech and Ernst (1998) interpreted the cuboid graphite aggregates to be pseudomorphs after diamond.

Direct evidence for the presence of diamond in this unit came from Raman spectroscopy. Bostick et al. (2003) identified what appeared to be three 2–3 μm cuboidal microdiamond inclusions in garnet from eclogite-facies gneiss. However, these "microdiamonds" were found to be nannocrystalline aggregates with SEM (scanning electron microscopy), which accounted for the broad spectral bands they displayed in Raman spectra. Based on these spectra and kinetic data for crystallization, Bostick et al. (2003) suggested that these diamonds formed at low temperatures relative to kimberlites or even the Kokchetav Massif (900–1000 °C).

Kairakli Unit

Garnet-clinopyroxene thermobarometry for mafic eclogite from the Kairakli unit yields equilibration temperatures ranging from 560 to 680 °C, and minimum pressure estimates of 1.5–2.6 GPa (Beane et al., 1995; Lennykh et al., 1995; Leech and Ernst, 2000). Similar temperature results were obtained from quartz-garnet-omphacite $\delta^{18}O$ equilibration in mafic eclogite and graphite-bearing schist, 595 to 711 °C (Leech and Ernst, 2000). The *P-T* conditions of 680 °C and 2.6 GPa calculated from garnet core and omphacite inclusion compositions plot adjacent to the quartz-coesite boundary (Fig. 4) (Bostick et al., 2003) and may be interpreted to reflect near-peak or possibly prograde conditions (Glodny et al., 2003), while the lower temperature and pressure estimates likely reflect retrograde conditions (Leech and Ernst, 1998). Oxygen isotope studies also indicated later retrograde reequilibration at ~453 ± 17 °C for the graphite schist (Leech and Ernst, 2000). This probably records the transitional blueschist/greenschist-facies metamorphism on the retrograde path (Fig. 4). Apparent $\delta^{18}O$ temperatures of ~250 ± 68 °C calculated for quartz-phengite pairs in metasedimentary rocks and a phengite-bearing eclogite suggest fluid-induced metasomatism and back-reaction during late-stage uplift (Leech and Ernst, 2000).

Yumaguzino Unit

The thermobarometric constraints for this unit remain tenuous. The presence of stilpnomelane suggests pressures less than 0.6 GPa (Miyano and Klein, 1989), but phengite Si contents up to 3.5 per formula unit suggest minimum pressures of 1.2 GPa (Hetzel et al., 1998). The occurrence of glaucophane also suggests blueschist-facies metamorphism (Beane and Connelly, 2000). Oxygen isotopes on quartz-albite and quartz-phengite pairs from the stilpnomelane quartzite show evidence that the rock equilibrated at ~453 ± 17 °C, showing the same transitional blueschist- to greenschist-facies metamorphism as the graphite-bearing schist in the Kairakli unit (Leech and Ernst, 2000).

Karamola Unit

The presence of lawsonite in mélange blocks of the Karamola unit suggests high-pressure, low-temperature metamorphism (Beane and Liou, 2005). Schulte and Sindern (2002) estimated peak *P-T* conditions of 1.8–2.1 GPa at ~520 °C if "average chlorite, Mg-rich garnet rim and average epidote compositions are used as equilibrium compositions of the former lawsonite assemblage" (Fig. 4). Oxygen isotope values for quartz-phengite pairs from a metasomatized basalt block show evidence that the rock reequilibrated at ~453 ± 17 °C. This temperature is evidence that the mélange of the Karamola unit underwent the same transitional blueschist/greenschist-facies metamorphism as graphite-bearing schist in the Kairakli unit and stilpnomelane quartzite of the Yumaguzino unit (Leech and Ernst, 2000). Pseudomorphic replacement of lawsonite by muscovite resulted from the influx of K-bearing fluid at *P-T* conditions around 0.4 GPa and 400 °C (Schulte and Sindern, 2002); the metasomatic event was followed by greenschist-facies metamorphism (Fig. 4) (Beane and Liou, 2005).

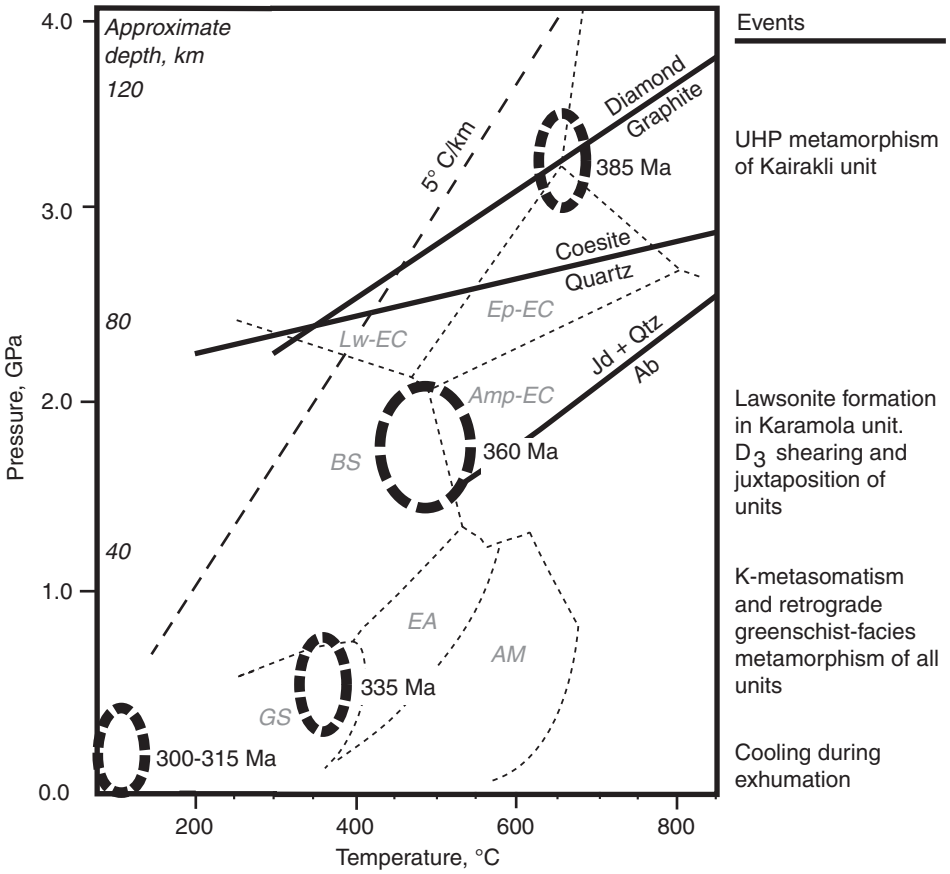

Figure 4. *P-T-t* path showing UHP metamorphism of the Kairakli unit (ca. 385 Ma), lawsonite formation in the Karamola unit and juxtaposition of all three units during blueschist-facies retrograde metamorphism in the Kairakli unit (ca. 360 Ma), K-metasomatism leading to pseudomorphism of lawsonite in the Karamola unit accompanied by greenschist-facies retrograde metamorphism of all units (ca. 335 Ma), and final exhumation (300–315 Ma). Ages from Table 1. Petrogenetic grid for metabasaltic bulk-rock compositions from Liou et al. (1998). Metamorphic facies abbreviations: AM—amphibolite; Amp-EC—amphibolite-eclogite; BS—blueschist; EA—epidote amphibolite; Ep-EC—epidote-eclogite; GS—greenschist; Lw-EC—lawsonite-eclogite.

STRUCTURAL EVOLUTION

The overall structure of the Maksyutov Complex is dominated by a northeast-southwest-trending foliation and gentle folding of all three units about asymmetrical fold axes parallel to the dominant foliation. This large-scale fabric resulted from the oblique convergence and the southeast-directed subduction of the leading edge of the East European platform (Fig. 1C) (Leech and Ernst, 2000). This paper reviews a structural history of four deformation stages (Hetzel et al., 1998; Hetzel, 1999). Although Dobretsov et al. (1996) delineated six stages of deformation, partly based on the work of Moskovchenko (1982), the four stages of deformation correspond more closely with our field observations and can be linked to metamorphic events.

Stages D_1–D_2

Stages D_1–D_2 are represented by a northeast-southwest foliation and intersection lineation and northwest-vergent folds (Fig. 5) (Hetzel et al., 1998; Leech and Ernst, 2000); these are interpreted to reflect progressive deformation stages that accompanied prograde metamorphism, i.e., formed during subduction (Hetzel et al., 1998). All three structures occur on field to thin-section scales (meso- to microscopic). Deformation is recorded best in the metasedimentary rocks of the Kairakli unit (cf. Leech and Ernst, 2000). Some mafic eclogite boudins appear to also exhibit an internal foliation that is interpreted to be a prograde feature by Hetzel et al. (1998). Alternatively, Leech and Ernst (2000) link the fabric to retrograde blueschist-facies metamorphism rather than prograde metamor-

Time Period for Major Tectonic Events	Radiometric Constraints	Deformation Events
LATEST PROTEROZOIC - MIDDLE CAMBRIAN Rifting and early plate break-up	Early to Middle Proterozoic ages for metasediments from the East European platform Latest Proterozoic to Middle Cambrian rift-related magmatism	
EARLY MIDDLE DEVONIAN (ca. 385 Ma) UHP metamorphism of the Maksyutov Complex	UHP metamorphism dated in eclogites and host metasediments dated with high-temperature chronometers between 390 and 380 Ma	D_1 - D_2 deformation: development of complex-wide NE-SW foliation and NW-vergent folds
MIDDLE DEVONIAN TO PENNSYLVANIAN (380-315 Ma) Exhumation and assembly of Maksyutov units	Multiple moderate- and low-temperature geochronometers date retrograde metamorphism (HP eclogite- to blueschist-facies) of Kairakli unit from 380-360 Ma All units yield dates between 370 and 340 Ma for retrograde metamorphism (blueschist- to greenschist-facies), metasomatism, and deformational events Greenschist-facies metamorphism of the Karamola unit between 330 and 340 Ma	D_3 shear zones developed between Kairakli and Karamola units and throughout the Yumaguzino during juxtaposition of units Exhumation-related D_4 shear zones and E-W stretching lineations develop corresponding to greenschist-facies metamorphism
PENNSYLVANIAN TO MIDDLE TRIASSIC (315-230 Ma) Cooling and continued convergence	Apatite fission-track data shows all 3 units cooled to 110°C (3-4 km depth) ca. 315 Ma Fission-track data indicates there was no significant displacement on the MUF after ca. 300 Ma	
PRESENT-DAY		

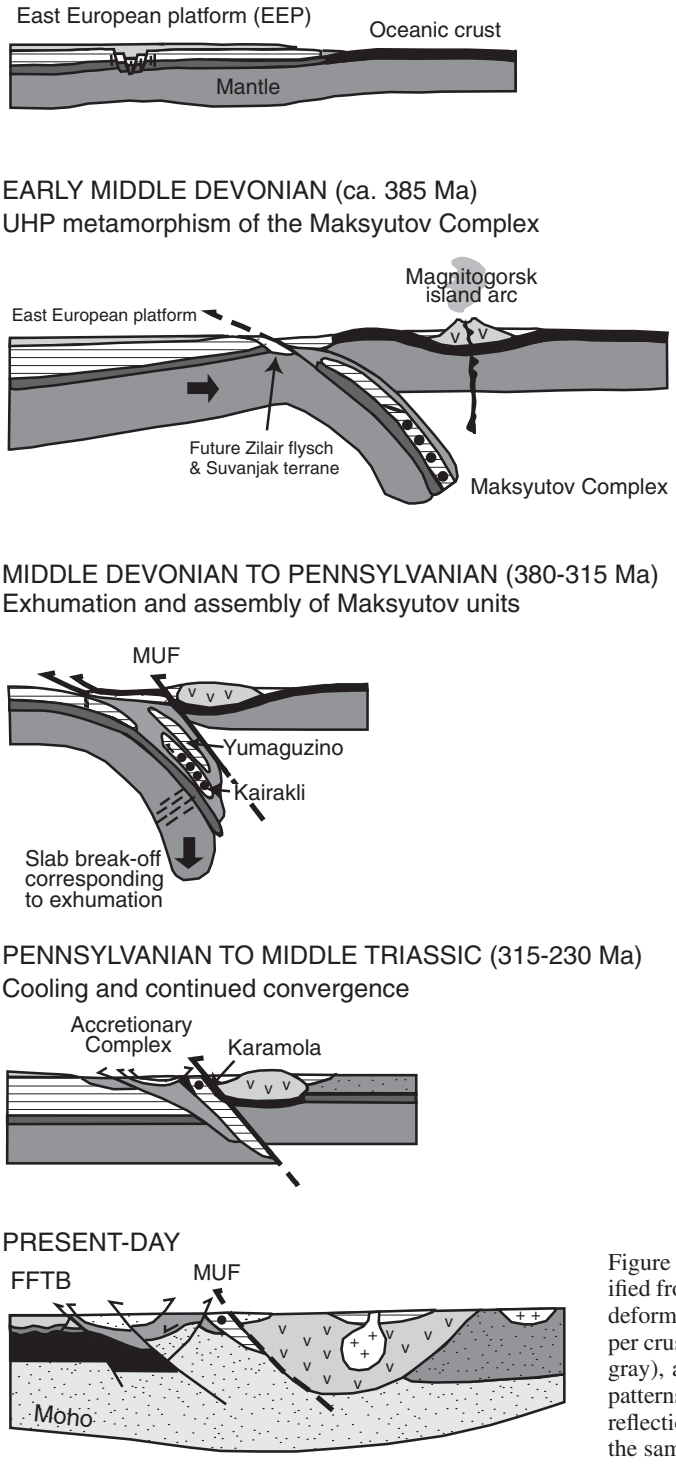

Figure 5. Model for the geodynamic evolution of the Maksyutov Complex (modified from Leech and Stockli, 2000) including radiometric dating constraints and deformational events. Early models show continental sediments (light gray), upper crust (horizontal lines), lower crust (dark gray), lithospheric mantle (medium gray), and oceanic crust (black); where identifiable, other tectonic units follow patterns in Figure 1B. The present-day crustal structure is adapted from seismic reflection data from Brown et al. (1998); patterns used for the present day are the same as in Figure 1B. Black dots represent the position of UHP rocks in the Kairakli unit. FFTB—foreland fold-and-thrust belt; MUF—Main Uralian fault.

phism. Hetzel et al. (1998) report weak deformation of some blocks of the Karamola unit "in the eastern limb of the Maksyutov Complex antiform" that these authors interpret as evidence for D_1–D_2 in that unit. The D_0–D_1 stages of Dobretsov et al. (1996) correspond to these stages. However, Dobretsov et al. (1996) emphasize that the deformation is observed only in metasedimentary rocks—not in mafic eclogites, and not in the Karamola unit.

Stage D_3

The D_3 stage of deformation is seen as a top-to-the-northeast ductile shear zone between the Kairakli and Karamola units (Fig. 1C) (Hetzel et al., 1998; Leech and Ernst, 2000), which also is well developed in the intervening Yumaguzino unit. The shear zone juxtaposed the Kairakli and Karamola units during exhumation to the *P-T* regime that produced transitional blueschist/greenschist-facies conditions (Fig. 5) (cf. Beane et al., 1995; Hetzel et al., 1998; Beane and Connelly, 2000; Leech and Ernst, 2000). In the Karayanova area, Leech and Ernst (2000) described a west-vergent thrust zone that juxtaposes the Kairakli and Yumaguzino units, which predates the shear zone between those units and the Karamola unit.

Stage D_4

The D_4 stage is represented by ductile shear zones and east-west stretching lineations at the margins of the complex (Fig. 1C) (Hetzel et al., 1998). It corresponds to stages D_5–D_6 of Dobretsov et al. (1996) that took place during retrograde greenschist-facies metamorphism. This deformation was produced by the exhumation of the Maksyutov Complex against the Suvanjak Complex to the west and the Magnitogorsk island arc to the east (Fig. 5).

GEOCHRONOLOGIC STUDIES

Geochronologic studies have helped to establish protolith, metamorphic, deformation, and cooling ages for the three units of the Maksyutov Complex (Table 1). These age data and their interpretations generally corroborate each other, but some interpretations differ, as highlighted below. Ascertaining various types of ages is critical in order to model exhumation rates, and place the evolution of the Maksyutov Complex within the tectonic framework of the Uralide orogen. (A summary of ages for the Uralide orogen is found in Scarrow et al., 2002.) Here, we discuss all the available geochronologic data from the original publications and reinterpret the age data in light of the entire body of work and current understanding of the evolution of the Maksyutov Complex.

Protolith Ages

Kairakli Unit

The Proterozoic protolith ages for metasedimentary rocks of the Kairakli unit indicate their origin as part of the East European platform. U-Pb SHRIMP (sensitive high-resolution ion microprobe) data from zircon cores yield a concordant age of 1778 ± 27 Ma (see GSA Data Repository[1]), nearly identical to the preliminary detrital zircon ages of 1800 ± 20 Ma reported by Krasnobaev et al. (1995) for magmatic zircon from metasedimentary rocks. Other studies have reported younger Precambrian ages (800 Ma to 1800 Ma; Table 1) for the protoliths of this unit (Dobretsov, 1974; Kozlov, 1982).

Recent U-Pb SHRIMP ages of zircons from the Kairakli unit range from the Middle Cambrian to the Early Ordovician (see GSA Data Repository; Leech and Willingshofer, 2004). These ages are consonant with the Early Ordovician age that Savielieva et al. (1997) assigned to the first magmatic event associated with the rifting of the East European platform and opening of the Uralian Ocean; alternatively, these ages could relate to postorogenic magmatism associated with the Timanian orogeny from ca. 550 to 490 Ma (Beckholmen and Glodny, 2004; Glodny et al., 2004). The age of rifting is based on conodonts in sedimentary rocks that are intercalated with basaltic lavas of ophiolites near the Main Uralian fault (Ivanov et al., 1989). Together, the protolith ages for Maksyutov Complex rocks, U-Th geochemistry of zircon (see GSA Data Repository), and geochemistry of the eclogites indicate that the mafic eclogite boudins formed as dikes and sills in older continental material during the initial opening of the Uralian Ocean.

Yumaguzino Unit

Krasnobaev et al. (1995) reported an upper intercept age of 1216 ± 93 Ma for detrital zircons of magmatic origin from the Yumaguzino unit.

Karamola Unit

Zircons from metasedimentary rocks in the Karamola unit record Proterozoic and Early Cambrian to Ordovician ages. U-Pb SHRIMP data for zircon cores yield two concordant Proterozoic ages (1417 ± 26 Ma and 1098 ± 18 Ma); eight zircons yield ages with weighted means of 520 ± 9 Ma and 548 ± 9 Ma (see GSA Data Repository). The similarity of protolith ages for metasedimentary rocks of both the Karamola and Kairakli units suggests they shared a common Proterozoic and early Paleozoic history. Marble lenses within the Karamola unit contain Late Silurian to Early Devonian conodonts (Puchkov, 1993). The Karamola meta-ophiolite may be older than the marble, based on one U-Pb zircon age of ca. 850 Ma (Valizer and Lennykh, 1988). Krasnobaev et al. (1995) attempted to date zircons from the meta-ophiolite but were unsuccessful.

Age of Peak Metamorphism

The age of peak metamorphism for the Kairakli unit has been much discussed. Dobretsov et al. (1996) and Coleman et al. (1993) suggested that UHP metamorphism took place at

[1]GSA Data Repository item 2007070, SHRIMP- RG age data, is available on the Web at http://www.geosociety.org/pubs/ft2007.htm. Requests may also be sent to editing@geosociety.org.

TABLE 1. SUMMARY OF GEOCHRONOLOGIC DATA FOR THE MAKSYUTOV COMPLEX

Age (Ma)	Method	Rock type	Location	Reference
Protolith ages				
1963–877	U-Pb zrn	Terrigenous		Kozlov (1982)
1800–443	U-Pb zrn	Metasediments	Kairakli unit	Krasnobaev et al. (1995)
1795–1144	U-Pb zrn	Metavolcanics		Dobretsov (1974)
1778 ± 27	U-Pb SHRIMP zrn	Metasedimentary	Kairakli unit	Leech and Willingshofer (2004)
1517–547	U-Pb zrn			Krasnobaev et al. (1995)
1417 ± 26	U-Pb SHRIMP zrn	Metasedimentary	Karamola unit	See GSA Data Repository
1216–352	U-Pb zrn	Quartzite	Yumaguzino unit	Krasnobaev et al. (1995)
1175–1077	Rb-Sr	Eclogite		Dobretsov (1974)
1098 ± 18	U-Pb SHRIMP zrn	Metasedimentary	Karamola unit	See GSA Data Repository
907–778	U-Pb zrn	Metavolcanics		Dobretsov (1974)
548 ± 9	U-Pb SHRIMP zrn	Metasedimentary	Karamola unit	See GSA Data Repository
532 ± 7	U-Pb SHRIMP zrn	Metasedimentary	Kairakli unit	Leech and Willingshofer (2004)
520 ± 9	U-Pb SHRIMP zrn	Metasedimentary	Karamola unit	See GSA Data Repository
514 ± 6	U-Pb SHRIMP zrn	Metasedimentary	Kairakli unit	Leech and Willingshofer (2004)
468	K-Ar WR	Diabase		Alekseyev (1976)
Peak metamorphism				
399 ± 35	Sm-Nd grt, rt, cpx, ap	Eclogite	Kairakli unit—Karayanova	Beane and Connelly (2000)
396 ± 57	Sm-Nd grt, cpx	Eclogite	Kairakli unit—Karayanova	Shatsky et al. (1997)
390 ± 20	K-Ar ms, WR	Metamorphic	Kairakli unit—Karayanova	Lennykh (1963)
388 ± 4	U-Pb SHRIMP zrn	Metasedimentary	Kairakli unit	Leech and Willingshofer (2004)
387.9 ± 4	$^{40}Ar/^{39}Ar$ wm	Blueschist	Kairakli unit	Matte et al. (1993)
384 ± 3	U-Pb rt	Eclogite	Kairakli unit—Karayanova	Beane and Connelly (2000)
382 ± 7	$^{40}Ar/^{39}Ar$ wm	Blueschist	Kairakli unit—Antigan	Hetzel and Romer (2000)
382 ± 10	Sm-Nd rt, ap	Eclogite	Kairakli unit—Karayanova	Beane and Connelly (2000)
379 ± 10	Rb-Sr WR wm	Blueschist	Kairakli unit—Antigan	Hetzel and Romer (2000)
378 ± 13	Sm-Nd WR	Eclogite	Kairakli unit	Shatsky et al. (1997)
Cooling ages and retrograde metamorphism				
377.7 ± 3.8	$^{40}Ar/^{39}Ar$ wm	Blueschist	Kairakli unit—Karayanova	Matte et al. (1993)
377 ± 2	$^{40}Ar/^{39}Ar$ phn	Graphite schist	Kairakli unit—Karayanova	Beane and Connelly (2000)
377 ± 2	U-Pb rt	Eclogite	Kairakli unit—Karayanova	Beane and Connelly (2000)
375.1 ± 1.8	Rb-Sr isochron WA	Eclogite	Kairakli unit	Glodny et al. (2002)
375.4 ± 1.7	$^{40}Ar/^{39}Ar$ wm	Eclogite	Kairakli unit—Karayanova	Lennykh et al. (1995)
375 ± 4	$^{40}Ar/^{39}Ar$ phn	Eclogite	Kairakli unit—Karayanova	Beane and Connelly (2000)
375 ± 3	Sm-Nd grt, cpx	Eclogite	Kairakli unit	Shatsky et al. (1997)
375 ± 2	$^{40}Ar/^{39}Ar$ wm		Kairakli unit—Karayanova	Lennykh et al. (1995)
374 ± 4	$^{40}Ar/^{39}Ar$ wm	Eclogite	Kairakli unit—Karayanova	Beane and Connelly (2000)
374 ± 3	$^{40}Ar/^{39}Ar$ phn	Eclogite	Kairakli unit—Shubino	Beane and Connelly (2000)
372.9 ± 3.8	$^{40}Ar/^{39}Ar$ wm	Eclogite	Kairakli unit—Karayanova	Matte et al. (1993)
372 ± 2	$^{40}Ar/^{39}Ar$ wm	Mica schist	Kairakli unit—Karayanova	Beane and Connelly (2000)
366 ± 7	Sm-Nd grt, cpx, wm	Eclogite	Kairakli unit—Karayanova	Shatsky et al. (1997)
357 ± 15	Sm-Nd grt, amp, zo		Kairakli unit—Karayanova	Shatsky et al. (1997)
357 ± 15	Sm-Nd grt, amp, zo		Kairakli unit—Karayanova	Shatsky et al. (1997)
Retrograde deformation in shear zones				
370 ± 7	$^{40}Ar/^{39}Ar$ wm	Qtz mylonite	Yumaguzino unit—Antigan	Hetzel and Romer (2000)
366 ± 12	Rb-Sr WR wm	Qtz mylonite	Yumaguzino unit—Antigan	Hetzel and Romer (2000)
365.5 ± 1.7	$^{40}Ar/^{39}Ar$	Quartzite	Kairakli unit—Karayanova	Lennykh et al. (1995)
365 ± 2	$^{40}Ar/^{39}Ar$	Eclogite	Kairakli unit—Karayanova	Lennykh et al. (1995)
365 ± 2	$^{40}Ar/^{39}Ar$ phn	Quartzite	Kairakli unit—Karayanova	Beane and Connelly (2000)
364 ± 7	$^{40}Ar/^{39}Ar$ wm	Qtz mylonite	Kairakli unit—Antigan	Hetzel and Romer (2000)
364 ± 4	Rb-Sr WR wm	Qtz mylonite	Karamola unit—Antigan	Hetzel and Romer (2000)
363 ± 10	Rb-Sr WR wm	Qtz mylonite	Yumaguzino unit—Antigan	Hetzel and Romer (2000)
359 ± 4	Rb-Sr WR wm	Qtz mylonite	Kairakli unit—Antigan	Hetzel and Romer (2000)
356 ± 7	$^{40}Ar/^{39}Ar$ wm	Qtz mylonite	Karamola unit—Antigan	Hetzel and Romer (2000)
358 ± 2	$^{40}Ar/^{39}Ar$ wm	Stilpnomelane qzt	Karamola unit—Karayanova	Beane and Connelly (2000)
356 ± 2	$^{40}Ar/^{39}Ar$ wm	Graphite quartzite	Yumaguzino unit—Karayanova	Beane and Connelly (2000)
352 ± 6	$^{40}Ar/^{39}Ar$ wm	Qtz mylonite	Kairakli unit—Antigan	Hetzel and Romer (2000)
344 ± 7	$^{40}Ar/^{39}Ar$ wm	Qtz mylonite	Yumaguzino unit—Antigan	Hetzel and Romer (2000)
K-metasomatism and formation of lawsonite pseudomorphs				
339 ± 6	Rb-Sr lws pseudomorph	Rodingite	Karamola unit—Utarbajevo	Schulte and Sindern (2002)
339 ± 2	$^{40}Ar/^{39}Ar$ ms	Metabasalt	Karamola unit—Karayanova	Beane and Connelly (2000)
338 ± 5	Rb-Sr lws pseudomorph	Rodingite	Karamola unit—Antigan	Schulte and Sindern (2002)
333 ± 2	$^{40}Ar/^{39}Ar$ wm	Quartzite	Karamola unit—Karayanova	Beane and Connelly (2000)
332 ± 3	$^{40}Ar/^{39}Ar$ ms	Metabasalt	Karamola unit—Novopakrova	Beane and Connelly (2000)
Apatite fission-track ages				
311 ± 45	fission-track ap	Metasomatite	Karamola unit—Karayanova	Leech and Stockli (2000)
261 ± 17	fission-track ap	Metasedimentary	Yumaguzino unit—Karayanova	Leech and Stockli (2000)
249 ± 15 to 265 ± 16	fission-track ap	Eclogite	Kairakli unit	Leech and Stockli (2000)
236 ± 14 to 262 ± 33	fission-track ap	Metasedimentary	Kairakli unit	Leech and Stockli (2000)
210 ± 12 to 275 ± 26	fission-track ap	Metasedimentary	Karamola unit	Leech and Stockli (2000)

Note: amp—amphibole; ap—apatite; cpx—clinopyroxene; grt—garnet; lws—lawsonite; ms—muscovite; phn—phengite; qtz—quartz; qzt—quartzite; rt—rutile; WA—weighted average; WR—whole rock; wm—white mica; zo—zoisite; zrn—zircon.

ca. 550 Ma, coeval with UHP metamorphism of the Kokchetav Massif. Subsequent data fail to support that model. Instead, several lines of evidence point to a ca. 385 Ma age for peak metamorphism (Table 1); this age is slightly older than the combined age estimate of 378 ± 6 Ma from Hetzel and Romer (2000), primarily because of the recently published SHRIMP work. Multiple studies using various isotopic systems have yielded overlapping ages between 380 and 390 Ma. The younger of these isotopic ages may date cooling during exhumation rather than peak metamorphism (Leech and Willingshofer, 2004; Hetzel and Romer, 2000; Beane and Connelly, 2000). However, the isotopic systems overlap and support a Middle Devonian age of peak metamorphism.

Ages for Retrograde Metamorphism, Deformation, and Cooling

The $^{40}Ar/^{39}Ar_{mica}$ data for the Kairakli unit yield ages from 365 to 382 Ma (Table 1). Closure temperatures for Ar in white micas (450° to 350 °C; Hanes, 1991; Monie, 1985) are below peak metamorphic temperatures, which means argon ages represent cooling upon exhumation (Beane and Connelly, 2000; Hetzel and Romer, 2000; Leech and Willingshofer, 2004). The 375–384 Ma $U\text{-}Pb_{rutile}$ ages also have been interpreted to be cooling ages (Leech and Willingshofer, 2004) based on an ~400 °C closure temperature (Mezger et al., 1989) for this system; other authors (Beane and Connelly, 2000; Hetzel and Romer, 2000) have interpreted these ages to reflect near-peak conditions, because the rutile closure temperature for the U-Pb system may be much higher (Santos Zalduegui et al., 1996). Rb-Sr mineral isochron data (Hetzel and Romer, 2000; Glodny et al., 2002) suggest a 375 ± 2 Ma age for eclogitization, but because this age corresponds to cooling using other thermochronometers (i.e., $^{40}Ar/^{39}Ar$ dating), we interpret the Rb-Sr data as postpeak metamorphism. Apatite fission-track data combined with $^{40}Ar/^{39}Ar_{mica}$ data indicate that the Kairakli unit cooled from ~400 °C to 110 °C between 375 and 315 Ma (Leech and Stockli, 2000).

The $^{40}Ar/^{39}Ar$ and Rb-Sr ages obtained from the D_3 and D_4 retrograde shear zones range from 370 to 344 Ma (Beane and Connelly, 2000; Hetzel and Romer, 2000), with a weighted age estimate of 360 ± 8 Ma (Hetzel and Romer, 2000). Most of the samples are from or from near the Yumaguzino unit. Hetzel and Romer (2000) and Beane and Connelly (2000) concluded that this dates the juxtaposition of the Maksyutov Complex units along the D_3 shear zone during exhumation to mid-crustal levels (blueschist/greenschist-facies metamorphism). In contrast, based on thermal modeling of the Maksyutov Complex, Leech and Willingshofer (2004) concluded that the blueschist/greenschist-facies overprint occurred in the lower crust (30 km depth).

The $^{40}Ar/^{39}Ar_{mica}$ data for the Karamola unit yield ages from 332 to 339 Ma (Table 1). The mica data were obtained from lawsonite pseudomorphs in equilibrium with chlorite (Schulte and Sindern, 2002; Beane and Liou, 2005). These ages represent a greenschist-facies metamorphism that postdated the shear zone (Beane and Connelly, 2000). Late-stage cooling is recorded by apatite fission-track data that indicate all three juxtaposed units cooled to 110 °C at 300 ± 25 Ma (Leech and Stockli, 2000).

EXHUMATION

Mechanism for Exhumation

Role of Normal Faulting

Unlike most other mountain belts, the Urals retain a collisional structure and did not undergo extensional collapse (Leech, 2001, and references therein); the Main Uralian fault constitutes the suture zone in the Urals and has never acted as a major extensional feature (although there was likely minor normal displacement along the Main Uralian fault late in the Uralian collision). This poses a problem explaining the exhumation of the Maksyutov Complex, which lies in the footwall of the Main Uralian fault; elsewhere, major bounding normal faults in UHP terranes (e.g., Dabie, China, and the Western Gneiss Complex, Norway) are used to model their exhumation (e.g., Hacker et al., 2000; Wang et al., 2000).

Echtler and Hetzel (1997) propose the Maksyutov Complex was exhumed by oblique thrusting on a fault west of the Zilair flysch to the west (see Fig. 1A), with coeval normal faulting on the Main Uralian fault. Evidence for exhumation along a basal thrust is based on syn-D_1-D_2 structures in the Maksyutov Complex and parallel fabrics in the Suvanjak Complex to the west (Fig. 1B). Hetzel et al. (1998) and Hetzel (1999) point to extensional shear zones and stretching lineations within the Maksyutov Complex that support exhumation by normal faulting on the Main Uralian fault.

Thermal modeling of the Maksyutov Complex suggests that normal faulting played only a minor role in exhumation (Leech and Willingshofer, 2004); even a small amount of normal displacement (2 mm/yr) on the Main Uralian fault forces the model to too low temperatures to fit the *P-T* path for the Maksyutov Complex. Fission-track data also suggest no normal motion on the Main Uralian fault after ca. 300 Ma because samples from the Maksyutov Complex and rocks in the Main Uralian fault hanging wall have a common thermal history (Leech and Stockli, 2000).

Buoyancy Forces

Buoyancy, an important force in UHP terranes, likely played a significant role exhuming the Maksyutov Complex. Like other UHP terranes, the total volume of mafic rocks (~3%) in the Maksyutov Complex is small compared to that of quartzofeldspathic rocks; as a result, this subducted crust is significantly more buoyant than the lower crust and upper mantle into which it is being subducted (Ernst et al., 1997; Ernst, 2001; Leech, 2001). Retrograde metamorphism of eclogite-facies rocks during exhumation can increase buoyancy as they are transformed to less-dense mineralogies. Additionally, the serpentinite mélange of the Main Uralian fault zone likely provided a weakened zone to aid the buoyant exhumation process (Guillot et al., 2000). Several

models for the geodynamic evolution of the Maksyutov Complex call for buoyant exhumation (Matte and Chemenda, 1996; Chemenda et al., 1997; Leech, 2001; Leech and Willingshofer, 2004). Given the evidence against major normal displacement on the Main Uralian fault, buoyancy was probably the major driving force for exhuming Maksyutov Complex rocks.

Exhumation Rate

Several attempts have been made at exhumation rate calculations for the UHP Kairakli unit simply using depth estimates and age data (e.g., 0.3–1.5 mm/yr [Leech and Stockli, 2000] to 2 mm/yr [Hetzel and Romer, 2000]). These very slow exhumation rates underestimate the true value because the calculations assume Maksyutov Complex rocks were at their deepest point in the subduction zone at ca. 375 Ma, which for some time was assumed to be the timing for peak metamorphism; recent, more accurate age dating (Leech and Willingshofer, 2004) has forced reinterpretation of the 375 Ma age (see Geochronologic Studies section) and, as a result, increases the exhumation rate.

Thermomechanical modeling shows that exhumation of Maksyutov Complex UHP rocks proceeded in multiple stages (Leech and Willingshofer, 2004). Leech and Willingshofer (2004) identified two, or perhaps three, distinct stages in the exhumation based on the rate at which the complex ascended: an initial moderate exhumation from UHP depths to the lower- to mid-crustal levels (30 km depth) at ~5 mm/yr followed by significantly slower exhumation to the upper crust (3–4 km depth) at a rate of ~0.5 mm/yr. This slowing is likely due to the decreasing contrasts in buoyancy forces as the Maksyutov Complex ascended through the crust. This moderate exhumation rate shows that in contrast to a widespread perception, fast exhumation is not required for the preservation of UHP minerals, though the Maksyutov Complex may represent the slow end member of UHP terranes.

Modeling

Based on earlier physical modeling for continental subduction, Chemenda et al. (1997) describes a low-compressional regime based on the total pull force of subducted lithosphere for the evolution of the Maksyutov Complex. The physical model predicts that when the subducted continental crust reaches a critical depth of 150 km, the subducted crust fails at depths of several tens of kilometers; this failure triggers the initial exhumation of the subducted crust (the Maksyutov Complex) and coincides with slab breakoff and the slowing of horizontal compression or collision.

Leech and Willingshofer (2004) performed modeling for the subduction and exhumation of the Kairakli unit to test the influence of various thermal and tectonic parameters in what may be a low-*P*-*T* end-member UHP complex; the modeling indicates that a relatively thin UHP unit (3–10 km), moderate exhumation rates (~5.0 mm/yr), and a small amount of cooling through continuing underthrusting of the cold subducting slab are required, and that radiogenic heat production must be low, to fit the *P*-*T*-*t* path (Fig. 4) of the Kairakli unit. This cooling could result from underthrusting of a cold footwall, normal displacement of hanging-wall units, or a combination of both; however, cooling through underthrusting was more efficient, and even small amounts of normal faulting along the Main Uralian fault meant the model could not reproduce the *P*-*T*-*t* path (Leech and Willingshofer, 2004).

GEODYNAMIC EVOLUTION

Combining the petrologic, thermobarometric, geochemical, and structural data with exhumation models and information regarding Uralide tectonics, we present a timeline for events that tie the evolution of the Maksyutov Complex with the development of the Uralide orogen (Fig. 5).

Proterozoic-Silurian

Metasediments from the Maksyutov Complex derive from East European platform sediments; detrital zircons from these units yield Proterozoic ages of 1100–1800 Ma (Krasnobaev et al., 1995; see GSA Data Repository). Rifting and the subsequent opening of the Uralian Ocean occurred from the Cambrian to Early Silurian based on the age of alkaline basalts, ophiolites, and graben-facies sediments (Ivanov et al., 1989; Savelieva et al., 1997; Maslov et al., 1997; Puchkov, 1997). The presence of deepwater turbidite sequences points to a rapidly deepening depression within the continental crust in the Sakmara zone, west of the Maksyutov Complex (Savelieva and Nesbitt, 1996). After the opening of the Uralian Ocean, the sedimentary protolith of the Maksyutov Complex formed the continental margin of the East European platform where it was intruded by basaltic dikes and sills; this rift-related magmatism is recorded in metabasaltic and metasedimentary rocks of the Kairakli and Karamola units (Volkova et al., 2004; Beane and Liou, 2005; this paper) that yield U-Pb zircon SHRIMP ages of ca. 510–550 Ma (Leech and Willingshofer, 2004; see GSA Data Repository).

Devonian

Eastward intraoceanic subduction commenced by the Silurian–earliest Devonian (Beane and Connelly, 2000; Leech and Willingshofer, 2004), resulting in thrust stacking of the East European platform margin and emplacement of oceanic crust (Leech and Willingshofer, 2004). The timing of the initiation of subduction is supported by the presence of ophiolitic fragments in the Late Silurian and Middle Devonian sequences of the Sakmara zone (Savelieva and Nesbitt, 1996) and Early Devonian volcanics of the Magnitogorsk arc (Spadea et al., 1997). Intraoceanic subduction ended with the closure of the Uralian Ocean by the earliest Devonian based on igneous crystallization ages for oceanic crust and timing of ophiolite emplacement along the suture zone (Edwards and Wasserburg, 1985; Leech and Willingshofer, 2004). Continental margin subduction fol-

lowed intraoceanic subduction; the edge of the former East European platform containing the protolith to Maksyutov Complex metasedimentary rock was subducted to great depths and metamorphosed at ultrahigh pressure ca. 385 Ma. Deformation stages D_1–D_2 in the Maksyutov Complex occurred during this subduction, resulting in northwest-vergent folding (Hetzel, 1999). Collision continued until the Late Devonian based on clastics in the Zilair flysch (Zonenshain et al., 1984).

Synconvergent buoyant exhumation (Chemenda et al., 1997; Leech and Willingshofer, 2004) of the UHP Kairakli unit from mantle depths to lower- to mid-crustal depths (blueschist/greenschist-facies conditions) took place in the Middle and Late Devonian, corresponding to evidence from fission-track dating (Leech and Stockli, 2000). Juxtaposition of the Kairakli, Yumaguzino, and Karamola units occurred in the Late Devonian (ca. 360 Ma) as evidenced by radiometric dating of minerals involved in D_3 shear zone deformation that developed at this time (Hetzel and Romer, 2000; Beane and Connelly, 2000).

Carboniferous-Tertiary

By the Early Carboniferous, subduction had ceased or at least slowed as indicated by the end of volcanic activity and the deposition of carbonates on the Magnitogorsk arc (Brown et al., 1998). By the Late Carboniferous, the Maksyutov Complex was exhumed to 10 km depth based on fission-track data modeling (Leech and Stockli, 2000). The exhumation of the Maksyutov Complex to upper-crustal levels occurred through buoyant uplift within the suture zone and by west-directed thrusting below (Echtler and Hetzel, 1997) and normal faulting (along the Main Uralian fault) above the complex (Chemenda et al., 1997), interposing it between the Suvanjak Complex to the west and the Magnitogorsk arc to the east. Deformational evidence for this exhumation is found in the greenschist-facies D_4 shear zones at the margins of the Maksyutov Complex (Hetzel, 1999). At the end of the Uralide orogen (ca. 230 Ma), rocks in the Maksyutov Complex underwent an episode of cooling (of ~40 °C) interpreted as erosional degradation of the orogen (Leech and Stockli, 2000). A regional marine transgression buried the area in the Jurassic and Cretaceous starting at ca. 180 Ma (Seward et al., 1997; Leech and Stockli, 2000). This was followed by a regional peneplanation and final exhumation to the surface at ca. 45 Ma (Leech and Stockli, 2000; Seward et al., 1997).

CONCLUSIONS

Nearly 40 years after Chesnokov and Popov (1965) first recognized radial fractures around quartz as possibly indicating the former presence of coesite, we now can call the Maksyutov Complex a UHP terrane based on the discovery of microdiamond by Bostick et al. (2003). This discovery builds on previous reports of UHP indicator minerals such as unconfirmed (by Raman spectroscopy) relict coesite (Dobretsov and Dobretsova, 1988) and graphite pseudomorphs after diamond (Leech and Ernst, 1998). In that same time, many workers in Russia and around the world have come to the south Urals and added greatly to the database of petrology, geochemistry, structure, and geochronology for the Maksyutov Complex.

Without a major extensional feature in the south Urals, buoyancy—resulting from vast density contrasts between subducted crust and the upper mantle—was a key mechanism in exhuming Maksyutov Complex rocks. While many workers invoke speedy exhumation to rapidly cool a UHP slab to avoid back-reaction of UHP index minerals, interpretations of the Maksyutov Complex suggest that fast exhumation is not a requirement. The rate estimate of 5 mm/yr for the Maksyutov Complex is much slower than most other UHP terranes: Exhumation rates for the Dabie Shan (eastern China) and Dora Maira Massif (European Alps) are on the order of 20–25 mm/yr (Gebauer et al., 1997; Webb et al., 1999), and new dating from Kaghan (Pakistan) suggests exhumation rates up to 90 mm/yr (Parrish et al., 2003). However, fast exhumation rates are not the most efficient mechanism to cool a UHP terrane (Peacock, 1995; Roselle and Engi, 2002; Leech and Willingshofer, 2004); the Maksyutov Complex was kept cool by continued subduction of cold crust during exhumation of a fairly thin (3–10 km) UHP slab (Leech and Willingshofer, 2004). The Maksyutov Complex is one of the most slowly exhumed, lowest-temperature UHP terranes; this provides us with important end-member conditions that may assist in modeling the exhumation of other UHP terranes.

The Uralide orogen is remarkably similar in terms of geology and crustal structure all along its 2500 km length. The Maksyutov Complex is not the only high-pressure belt in this mountain chain—there are many other eclogite-bearing subduction complexes (e.g., Puchkov, 1989); perhaps given the difficulty in proving UHP metamorphism in the Maksyutov Complex, we should revisit those areas to hunt for mineralogical evidence. Coesite and/or diamond now has been found along the entire Qinling-Dabie-Sulu orogen in China (Yang et al., 2001); if the tectonic processes that formed the Maksyutov Complex were also continuous along the Ural Mountains, perhaps it could end up being the world's longest UHP orogen.

ACKNOWLEDGMENTS

This paper is dedicated to Gary Ernst, our former graduate advisor, who for decades has enthusiastically motivated students and colleagues toward recognizing and modeling the subduction and exhumation of high-pressure, low-temperature terranes. Research leading to this paper has been supported in part by National Science Foundation (NSF) grants EAR-9304480 to R.G. Coleman, EAR-9725347 to J.G. Liou, OISE-99001573 to M.L., NSF graduate fellowships to R.B. and M.L., and funding from Bowdoin College and Stanford University. We are grateful to R.G. Coleman, W.G. Ernst, J.G. Liou, V. Lennykh (deceased), P. Valizer, and R. Zhang for assistance in the field and continued discussions. S. Sorensen, J. Glodny, and an anonymous reviewer provided constructive feedback during the review.

REFERENCES CITED

Alekseev, A.A., 2000, Graphite eclogite from the Maksyutov Complex metamorphic complex, southern Urals: Doklady Earth Sciences, v. 372, p. 669–671.

Alekseyev, A.A., 1976, New data of the stratigraphy of the Maksyutov Complex metamorphic complex, southern Urals: Doklady Earth Sciences, v. 227, p. 41–44.

Alekseyev, A.A., Alekseyeva, G.V., and Yevdokimova, Z.V., 1978, Chromium phengite in metamorphic rocks of the Maksyutov Complex, southern Urals, *in* Tamarinov, P.M., ed., Mineraly i paragenezisy mineralov, USSR: Izd. Nauka, Leningrad, USSR, p. 141–143 (in Russian).

Bea, F., Fershtater, G.B., and Montero, P., 2002, Granitoids of the Uralides: Implications for the evolution of the orogen, *in* Brown, D., et al., eds., Mountain building in the Uralides: Pangea to present: American Geophysical Union Geophysical Monograph 132, p. 211–232.

Beane, R.J., and Connelly, J.N., 2000, $^{40}Ar/^{39}Ar$, U-Pb, and Sm-Nd constraints on the timing of metamorphic events in the Maksyutov Complex southern Ural Mountains: Geological Society [London] Journal, v. 157, p. 811–822.

Beane, R.J., and Liou, J.G., 2005, Metasomatism in serpentinite mélange rocks from the high-pressure Maksyutov Complex, southern Ural Mountains, Russia: International Geology Review, v. 47, p. 24–40.

Beane, R.J., Liou, J.G., Coleman, R.G., and Leech, M.L., 1995, Mineral assemblages and retrograde *P-T* path for high- to ultrahigh-pressure metamorphism in the lower unit of the Maksyutov Complex, southern Ural Mountains, Russia: Island Arc, v. 4, p. 254–266, doi: 10.1111/j.1440-1738.1995.tb00148.x.

Beckholmen, M., and Glodny, J., 2004, Timanian blueschist-facies metamorphism in the Kvarkush metamorphic basement, northern Urals, Russia, *in* Gee, D.G., and Pease, V., eds., The Neoproterozoic Timanide orogen of eastern Baltica: Geological Society [London] Memoir 30, p. 125–134.

Berzin, R., Oncken, O., Knapp, J.H., Perez-Estaun, A., Hismatulin, T., Yunusov, N., and Lipilin, A., 1996, Orogenic evolution of the Ural Mountains: Results from an integrated seismic experiment: Science, v. 274, p. 220–221, doi: 10.1126/science.274.5285.220.

Bostick, B., Jones, R.E., Ernst, W.G., Chen, C., Leech, M.L., and Beane, R.J., 2003, Low-temperature microdiamond aggregates in the Maksyutov Complex metamorphic complex, south Ural Mountains, Russia: American Mineralogist, v. 88, p. 1709–1717.

Brown, D., and Spadea, P., 1999, Processes of forearc and accretionary complex formation during arc-continent collision in the southern Ural Mountains: Geology, v. 27, p. 649–652, doi: 10.1130/0091-7613(1999)027<0649:POFAAC>2.3.CO;2.

Brown, D., Juhlin, C., Alvarez-Marron, J., Pérez-Estaún, A., and Oslianski, A., 1998, Crustal-scale structure and evolution of an arc-continent collision zone in the southern Urals, Russia: Tectonics, v. 17, p. 158–171, doi: 10.1029/98TC00129.

Carbonell, R., Perez-Estaun, A., Gallart, J., Diaz, J., Kashubin, S., Mechie, J., Stadtlander, R., Schulze, A., Knapp, J., and Mrozov, A., 1996, A crustal root beneath the Urals: Wide-angle seismic evidence: Science, v. 274, p. 222–224, doi: 10.1126/science.274.5285.222.

Chemenda, A., Matte, P., and Sokolov, V., 1997, A model of Palaeozoic obduction and exhumation of high-pressure/low-temperature rocks in the southern Urals: Tectonophysics, v. 276, p. 217–227, doi: 10.1016/S0040-1951(97)00057-7.

Chesnokov, B.V., and Popov, V.A., 1965, Increasing volume of quartz grains in eclogites of the south Urals: Doklady Akademii Nauk SSSR, v. 162, p. 176–178.

Chibrikova, Y.V., and Olli, V., 1994, The finds of acritarchs from the metamorphic complex of the Ural-Tau range: A way to better knowledge and use the Bashkortostan Interior: Bashkortostan, Ufa Academy of Science, p. 1–51 (in Russian).

Chopin, C., 1984, Coesite and pure pyrope in high-grade blueschist of the western Alps: A first record and some consequences: Contributions to Mineralogy and Petrology, v. 86, p. 107–118, doi: 10.1007/BF00381838.

Coleman, R.G., and Wang, X., 1995, Ultrahigh-pressure metamorphism: New York, Cambridge University Press, 528 p.

Coleman, R.G., Liou, J.G., Zhang, R.Y., Dobretsov, N., Shatsky, V., and Lennykh, V., 1993, Tectonic setting of the UHPM Maksyutov Complex, Ural Mountains, Russia: Eos (Transactions, American Geophysical Union), v. 74, p. 47.

Dobretsov, N.L., 1974, Glaucophane schists and eclogite glaucophane-schist complexes in the USSR: Novosibirsk, Nauka, p. 1–429 (in Russian).

Dobretsov, N.L., and Dobretsova, L.V., 1988, New mineralogical data on the Maksyutov Complex eclogite-glaucophane schist complex, southern Urals: Doklady Akademii Nauk SSSR, v. 300, p. 111–116.

Dobretsov, N.L., Shatsky, V.S., Coleman, R.G., Lennykh, V.I., Valizer, P.M., Liou, J.G., Zhang, R., and Beane, R.J., 1996, Tectonic setting and petrology of ultrahigh-pressure metamorphic rocks in the Maksutov Complex, Ural Mountains, Russia: International Geology Review, v. 38, p. 136–160.

Echtler, H.P., 1996, Paleozoic non-extensional exhumation of the Maksiutova HP belt, southern Urals: Eos (Transactions, American Geophysical Union), v. 77, p. 766.

Echtler, H.P., and Hetzel, R., 1997, Main Uralian Thrust and Main Uralian Normal Fault: Non-extensional Paleozoic high-*P* rock exhumation, oblique collision, and normal faulting in the southern Urals: Terra Nova, v. 9, p. 158–162, doi: 10.1046/j.1365-3121.1997.d01-27.x.

Edwards, R.L., and Wasserburg, G.J., 1985, The age and emplacement of obducted oceanic crust in the Urals from Sm-Nd and Rb-Sr systematics: Earth and Planetary Science Letters, v. 72, p. 389–404, doi: 10.1016/0012-821X(85)90060-3.

Ernst, W.G., 2001, Subduction, ultrahigh-pressure metamorphism, and regurgitation of buoyant crustal slices—Implications for arcs and continental growth: Physics of the Earth and Planetary Interiors, v. 127, p. 253–275, doi: 10.1016/S0031-9201(01)00231-X.

Ernst, W.G., and Liou, J.G., 2000, Ultrahigh-pressure metamorphism and geodynamics in collision-type orogenic belts: Geological Society of America, International Book Series, v. 4, 293 p.

Ernst, W.G., Maruyama, S., and Wallis, S., 1997, Buoyancy-driven, rapid exhumation of ultrahigh-pressure metamorphosed continental crust: Proceedings of the National Academy of Sciences of the United States of America, v. 94, p. 9532–9537, doi: 10.1073/pnas.94.18.9532.

Gebauer, D., Schertl, H.-P., Brix, M., and Schreyer, W., 1997, 35 Ma old ultrahigh-pressure metamorphism and evidence for rapid exhumation in the Dora Maira Massif, western Alps: Lithos, v. 41, p. 5–24, doi: 10.1016/S0024-4937(97)82002-6.

Glodny, J., Bingen, B., Austrheim, H., Molina, J.F., and Rusin, A., 2002, Precise eclogitization ages deduced from Rb/Sr mineral systematics: The Maksyutov Complex, southern Urals, Russia: Geochimica et Cosmochimica Acta, v. 66, p. 1221–1235, doi: 10.1016/S0016-7037(01)00842-0.

Glodny, J., Austrheim, H., Molina, J.F., Rusin, A.I., and Seward, D., 2003, Rb/Sr record of fluid-rock interaction in eclogites: The Marun-Keu Complex, polar Urals, Russia: Geochimica et Cosmochimica Acta, v. 67, p. 4353–4371, doi: 10.1016/S0016-7037(03)00370-3.

Glodny, J., Pease, V., Montero, P., Austrheim, H., and Rusin, A.I., 2004, Protolith ages of eclogites, Marun-Keu Complex, polar Urals, Russia: Implications for the pre- and early Uralian evolution of the northeastern European continental margin, *in* Gee, D.G., and Pease, V., eds., The Neoproterozoic Timanide orogen of eastern Baltica: Geological Society [London] Memoir 30, p. 87–105.

Gorochov, S.S., and Chabakov, A.W., 1961, Geologic map M-40-IV (central Maksyutov Complex): South Urals Series, scale 1:200,000 (in Russian).

Guillot, S., Hattori, K.H., and de Sigoyer, J., 2000, Mantle wedge serpentinization and exhumation of eclogites: Insights from eastern Ladakh, northwest Himalaya: Geology, v. 28, p. 199–202, doi: 10.1130/0091-7613(2000)028<0199:MWSAEO>2.3.CO;2.

Hacker, B.R., and Liou, J.G., 1998, When continents collide: Geodynamics and geochemistry of ultrahigh-pressure rocks: Boston, Kluwer Academic Publishers, 323 p.

Hacker, B.R., Ratschbacher, L., Webb, L., McWilliams, M.O., Ireland, T., Calvert, A., Dong, S., Wenk, H.R., and Chateigner, D., 2000, Exhumation of ultrahigh-pressure continental crust in east-central China: Late Triassic–Early Jurassic tectonic unroofing: Journal of Geophysical Research, v. 105, p. 13,339–13,364, doi: 10.1029/2000JB900039.

Hamilton, W., 1970, The Uralides and the motion of the Russian and Siberian platforms: Geological Society of America Bulletin, v. 81, p. 2553–2576.

Hanes, J.A., 1991, K-Ar and $^{40}Ar/^{39}Ar$ Geochronology: Methods and applications, *in* Heaman, L., and Ludden, J.N., eds., Applications of radiogenic isotope systems to problems in geology: Mineralogical Association of Canada, Short Course Handbook, v. 19, p. 27–57.

Hetzel, R., 1999, Geology and geodynamic evolution of the high-*P*/low-*T* Maksyutov Complex, southern Urals, Russia: Geologische Rundschau, v. 87, p. 577–588, doi: 10.1007/s005310050232.

Hetzel, R., and Romer, R.L., 2000, A moderate exhumation rate for the high-pressure Maksyutov Complex, southern Urals, Russia: Geological Journal, v. 35, p. 327–344, doi: 10.1002/gj.862.

Hetzel, R., Echtler, H.P., Seifert, W., Schulte, B.A., and Ivanov, K.S., 1998, Subduction- and exhumation-related fabrics in the Paleozoic high-pressure–low-temperature Maksyutov Complex, Antingan area, southern Urals, Russia: Geological Society of America Bulletin, v. 110, p. 916–930, doi: 10.1130/0016-7606(1998)110<0916:SAERFI>2.3.CO;2.

Ivanov, K.S., Puchkov, V.N., Nadedkina, V.A., and Pelevin, L.A., 1989, First results on revised stratigraphy of the Polyakovka Formation based on conodonts, *in* Exhegodnik-88: Sverdlovsk, Institute of Geology and Geochemistry, Uralian Department, Russian Academy of Sciences, p. 12–13 (in Russian).

Klochichin, A.V., and Burychenko, A.B., 1957, Geologic map (southern Maksyutov Complex): South Urals Series M-40-IV, scale 1:200,000 (in Russian).

Knapp, H.H., Diaconescu, M.A., Bader, M.A., Sokolov, V.B., Kashubin, S.N., and Rybalka, A.V., 1998, Seismic reflection fabrics of continental collision and post-orogenic extension in the middle Urals, central Russia: Tectonophysics, v. 288, p. 115–126, doi: 10.1016/S0040-1951(97)00288-6.

Kozlov, V.I., 1982, Upper Riphean and Vendian of the southern Urals: Moscow, Nauka, 128 p. (in Russian).

Krasnobaev, A.A., Davudov, B.A., Lennykh, V.I., Tscherednitschencko, N.B., and Kosolov, W.J., 1995, The ages of zircons and rutiles from the Maksyutov Complex (preliminary data): Ekaterinburg, Yearbook 1995, Uralian Russian Academy of Sciences, p. 13–16 (in Russian).

Kretz, R., 1983, Symbols for rock-forming minerals: American Mineralogist, v. 68, p. 277–279.

Krinizky, D.D., and Krinizkaya, W.M., 1961, Stratigraphy of metamorphic sequences along the middle part of the Sakmara River: Sakmari Materiali po geologii Yuznago Urala, v. 67, p. 167–174 (in Russian).

Leech, M.L., 2001, Arrested orogenic development: Eclogitization, delamination, and tectonic collapse: Earth and Planetary Science Letters, v. 185, p. 149–159, doi: 10.1016/S0012-821X(00)00374-5.

Leech, M.L., and Ernst, W.G., 1998, Graphite pseudomorphs after diamond? A carbon isotope and spectroscopic study of graphite cuboids from the Maksyutov Complex, south Ural Mountains, Russia: Geochimica et Cosmochimica Acta, v. 62, p. 2143–2154.

Leech, M.L., and Ernst, W.G., 2000, Petrotectonic evolution of the high- to ultrahigh-pressure Maksyutov Complex, Karayanova area, south Ural Mountains, Russia: Structural and oxygen isotopic constraints: Lithos, v. 52, p. 235–252, doi: 10.1016/S0024-4937(99)00093-6.

Leech, M.L., and Stockli, D.F., 2000, The late exhumation history of the ultrahigh-pressure Maksyutov Complex, south Ural Mountains, from new apatite fission track data: Tectonics, v. 19, p. 153–167, doi: 10.1029/1999TC900053.

Leech, M.L., and Willingshofer, E., 2004, Thermal modeling of an ultrahigh-pressure complex in the south Urals: Earth and Planetary Science Letters, v. 226, p. 85–99, doi: 10.1016/j.epsl.2004.07.009.

Lennykh, V.I., 1963, O vozraste metamorficheskikh porod zony Uraltau, Akademii Nauk SSSR: Komisii po opredelenyo absolyutovo vozrasta geologicheskii formatsii, v. 11, p. 253–264.

Lennykh, V.I., 1977, Eclogite-glaucophane belt of south Urals: Moscow, Nauka, 158 p. (in Russian).

Lennykh, V.I., and Valizer, P.M., 1986, Lawsonite rodingite of the Maksyutov Complex eclogite-glaucophane schist complex: Geologii and Geochemii, p. 73–76 (in Russian).

Lennykh, V.I., Valizer, P.M., Beane, R.J., Leech, M.L., and Ernst, W.G., 1995, Petrotectonic evolution of the Maksyutov Complex, south Urals, Russia: Implications for ultrahigh-pressure metamorphism: International Geology Review, v. 37, p. 584–600.

Liou, J.G., Zhang, R., and Ernst, W.G., 1994, An introduction to ultrahigh-pressure metamorphism: Island Arc, v. 3, p. 1–24, doi: 10.1111/j.1440-1738.1994.tb00001.x.

Liou, J.G., Zhang, R.Y., Ernst, W.G., Rumble, D., III, and Maruyama, S., 1998, High-pressure minerals from deeply subducted metamorphic rocks: Reviews in Mineralogy, v. 37, p. 33–96.

Liou, J.G., Tsujimori, T., Zhang, R.Y., Katayama, I., and Maruyama, S., 2004, Global UHP metamorphism and continental subduction/collision: The Himalayan model: International Geology Review, v. 46, p. 1–27.

Lodochnikov, V.N., 1941, The first lawsonite in the Soviet Union (an attempt to characterize the rock-forming minerals): Izvestiya Akademii Nauk SSSR, seriya geologicheskaya, v. 1, p. 125–140 (in Russian).

Maslov, A.V., Erdtmann, B.D., Ivanov, K.S., Ivanov, S.N., and Krupenin, M.T., 1997, The main tectonic events, depositional history, and the palaeogeography of the southern Urals during the Riphean–early Palaeozoic: Tectonophysics, v. 276, p. 313–335, doi: 10.1016/S0040-1951(97)00064-4.

Matte, P., and Chemenda, A., 1996, A mechanism for exhumation of high-pressure metamorphic rocks during continental subduction in southern Urals: Comptes Rendus de l'Académie des Sciences, Serie II, v. 323, p. 525–530.

Matte, P., Maluski, H., Caby, R., Nicholas, A., Kepezhinkskas, P., and Sobolev, S., 1993, Geodynamic model and $^{39}Ar/^{40}Ar$ dating for the generation and emplacement of the high-pressure metamorphic rocks in SW Urals: Comptes Rendus de l'Académie des Sciences, Serie II, v. 317, p. 1667–1674.

Mezger, K., Hanson, G.N., and Bohlen, S.R., 1989, High-precision U-Pb ages of metamorphic rutile: Application to the cooling history of high-grade terranes: Earth and Planetary Science Letters, v. 96, p. 106–118, doi: 10.1016/0012-821X(89)90126-X.

Miyano, T., and Klein, C., 1989, Phase equilibria in the system K_2O-FeO-MgO-Al_2O_3-SiO_2-H_2O-CO_2 and the stability limit of stilpnomelane in the metamorphosed Precambrian iron-formations: Contributions to Mineralogy and Petrology, v. 102, p. 478–491, doi: 10.1007/BF00371089.

Monie, P., 1985, The ^{39}Ar-^{40}Ar method applied to Alpine metamorphism in the Monte Rosa Massif (western Alps): Detailed chronology since 100 Ma: Eclogae Geologicae Helvetiae, v. 78, p. 487–516.

Moskovchenko, N.I., 1982, Precambrian high-pressure complexes in Phanerozoic folded belts: Moscow, Nauka, 161 p. (in Russian).

Parrish, R.R., Gough, S., Searle, M., and Waters, D., 2003, Exceptionally rapid exhumation of the Kaghan UHP terrane, Pakistan, from U-Th-Pb measurements on accessory minerals: Geological Society of America Abstracts with Programs, v. 35, no. 6, p. 556.

Peacock, S.M., 1995, Ultrahigh-pressure metamorphic rocks and the thermal evolution of continent collision belts: Island Arc, v. 4, p. 376–383, doi: 10.1111/j.1440-1738.1995.tb00157.x.

Puchkov, V.N., 1989, The collisional origin of the eclogite-glaucophane-schist belt of the Urals: Ofioliti, v. 14, p. 213–220.

Puchkov, V.N., 1993, The paleo-oceanic structures of the Ural Mountains: Geotectonics, v. 27, p. 184–196.

Puchkov, V.N., 1997, Structure and geodynamics of the Uralian orogen, *in* Burg, J.P., and Ford, M., eds., Orogen through time: Geological Society [London] Special Publication 121, p. 201–236.

Roselle, G.T., and Engi, M., 2002, Ultra-high-pressure (UHP) terrains: Lessons from thermal modeling: American Journal of Science, v. 302, p. 410–441, doi: 10.2475/ajs.302.5.410.

Santos Zalduegui, J.F.S., Scharer, U., Ibarguchi, J.I.G., and Girardeau, J., 1996, Origin and evolution of the Paleozoic Cabo Ortegal ultramafic-mafic complex (NW Spain): U-Pb, Rb-Sr, and Pb-Pb isotope data: Chemical Geology, v. 129, p. 281–304, doi: 10.1016/0009-2541(95)00144-1.

Savelieva, G.N., and Nesbitt, R.W., 1996, A synthesis of the stratigraphic and tectonic setting of the Uralian ophiolites: Geological Society [London] Journal, v. 153, p. 525–537.

Savelieva, G.N., Sharaskin, Q.Y., Saveliev, A.A., Spadea, P., and Gaggero, L., 1997, Ophiolites of the southern Uralides adjacent to the East European continental margin: Tectonophysics, v. 276, p. 117–137, doi: 10.1016/S0040-1951(97)00053-X.

Scarrow, J.H., Hetzel, R., Gorozhanin, V.M., Dinn, M., Gldny, J., Gerdes, A., Ayala, C., and Montero, P., 2002, Four decades of geochronological work in the southern and middle Urals: A review in mountain building in the Uralides: Pangea to the Present: American Geophysical Union Geophysical Monograph 132, p. 233–255.

Schulte, B.A., and Blümel, P., 1999, Metamorphic evolution of eclogite and associated garnet-mica schist in the high-pressure metamorphic Maksyutov Complex, Ural, Russia: Geologische Rundschau, v. 87, p. 561–576, doi: 10.1007/s005310050231.

Schulte, B., and Sindern, S., 2002, K-rich fluid metasomatism at high-pressure metamorphic conditions: Lawsonite decomposition in rodingitized ultramafite of the Maksyutov Complex, southern Urals (Russia): Journal of Metamorphic Geology, v. 20, p. 529–541, doi: 10.1046/j.1525-1314.2002.00387.x.

Seward, D., Perez-Estaun, A., and Puchkov, V., 1997, Preliminary fission-track results from the southern Urals: Sterlitamak to Magnitogorsk: Tectonophysics, v. 276, p. 281–290, doi: 10.1016/S0040-1951(97)00061-9.

Shatsky, V.S., Jagoutz, E., and Koz'menko, O.A., 1997, Sm-Nd dating of the high-pressure metamorphism of the Maksyutov Complex, southern Urals: Transactions of the Russian Academy of Sciences, Earth Science Section, v. 353, p. 285–288.

Smith, D.C., 1984, Coesite in clinopyroxene in the Caledonides and its implications for geodynamics: Nature, v. 310, p. 641–644, doi: 10.1038/310641a0.

Spadea, P., Kabanova, L., and Gaggero, L., 1997, Trace element characteristics of Mid-Devonian boninitic rocks from the Bruibai zone, southern Urals: EUG (European Union of Geosciences), v. 9, p. 126.

Valizer, P.M., and Lennykh, V.I., 1988, Amphiboles of blueschists of the Urals: Moscow, Nauka, 202 p. (in Russian).

Volkova, N.I., Frenkel, A.E., Budanov, V.I., and Lepezin, G.G., 2004, Geochemical signatures for eclogite protoliths from the Maksyutov Complex, south Urals: Journal of Asian Earth Sciences, v. 23, p. 745–759, doi: 10.1016/S1367-9120(03)00128-7.

Wang, C.Y., Zeng, R.S., Mooney, W.D., and Hacker, B.R., 2000, A crustal model of the profiling: Journal of Geophysical Research, v. 105, p. 10,857–10,869.

Webb, L.E., Hacker, B.R., Ratschbacher, L., McWilliams, M.O., and Dong, S.W., 1999, Thermochronologic constraints on deformation and cooling history of high- and ultrahigh-pressure rocks in the Qinling-Dabie orogen, eastern China: Tectonics, v. 18, p. 621–638, doi: 10.1029/1999TC900012.

Yang, S.S., Xu, Z., Song, S., Zhang, J., Wu, C., Shi, R., Li, H., and Brunel, M., 2001, Discovery of coesite in the north Qaidam early Palaeozoic ultrahigh-pressure (UHP-HP) metamorphic belt, NW China: Comptes Rendus de l'Académie des Sciences, Serie II, Sciences de la Terre et des Planetes, v. 333, p. 719–724.

Zonenshain, L.P., Korinevsky, V.G., Kazmin, V.G., Pecherskiy, D.M., Khain, V.V., and Matveyenkov, V.V., 1984, Plate tectonic model of the south Urals development: Tectonophysics, v. 109, p. 95–135, doi: 10.1016/0040-1951(84)90173-2.

Zonenshain, L.P., Kuzmin, M.I., and Natapov, L.M., 1990, Geology of the USSR: A plate-tectonic synthesis, *in* Page, B.M., ed., Geology of the USSR: A plate-tectonic synthesis: American Geophysical Union Geodynamics Series, v. 21, 242 p.

Manuscript Accepted by the Society 13 July 2006